

Effects of the individual particle relaxation time on superspin glass dynamicsMikael Svante Andersson,^{1,*} Jose Angel De Toro,² Su Seong Lee,³ Peter S. Normile,² Per Nordblad,¹ and Roland Mathieu¹¹*Department of Engineering Sciences, Uppsala University, Box 534, SE-751 21 Uppsala, Sweden*²*Instituto Regional de Investigación Científica Aplicada (IRICA) and Departamento de Física Aplicada, Universidad de Castilla-La Mancha 13071 Ciudad Real, Spain*³*Institute of Bioengineering and Nanotechnology, 31 Biopolis Way, The Nanos, Singapore 138669, Singapore*

(Received 21 December 2015; published 8 February 2016)

The low temperature dynamic magnetic properties of two dense magnetic nanoparticle assemblies with similar superspin glass transition temperatures $T_g \sim 140$ K are compared. The two samples are made from batches of 6 and 8 nm monodisperse γ -Fe₂O₃ nanoparticles, respectively. The properties of the individual particles are extracted from measurements on reference samples where the particles have been covered with a thick silica coating. The blocking temperatures of these dilute assemblies are found at 12.5 K for the 6 nm particles and at 35 K for the 8 nm particles, which implies different anisotropy energy barriers of the individual particles and vastly different temperature evolution of their relaxation times. The results of the measurements on the concentrated particle assemblies suggest a strong influence of the particle energy barrier on the details of the aging dynamics, memory behavior, and apparent superspin dimensionality of the particles.

DOI: [10.1103/PhysRevB.93.054407](https://doi.org/10.1103/PhysRevB.93.054407)**I. INTRODUCTION**

The effect of magnetic anisotropy energy, $E_a = KV$, where K is the anisotropy constant and V the particle volume, is well understood for magnetic nanoparticles in dilute systems where E_a governs the relaxation time, τ , of the particle [1]. The temperature dependence of τ is described by the Arrhenius law $\tau = \tau_0 \exp(KV/k_B T)$ [2], where τ_0 is the relaxation time at high temperatures T . The temperature evolution of τ also determines the blocking temperature, T_b , which can be defined as the temperature of the maximum in low field ac susceptibility or zero field cooled (ZFC) dc magnetization as a function of temperature.

For highly concentrated particle systems, however, collective phenomena are introduced with spin-glass-like dynamics due to the frustration induced by the interparticle interactions between randomly located NPs [3–6]. These systems are therefore called superspin glasses, adopting the nomenclature from superparamagnetism [1,3]. For interactions greater than the NPs individual anisotropy barriers, the glass transition has been suggested to depend solely on the strength of the interparticle interactions [7,8].

In this article we investigate the low field magnetic properties of very dilute (magnetically isolated particles) and highly concentrated (strongly interacting particles) samples both comprising assemblies of monodisperse γ -Fe₂O₃ NPs. Two different maghemite particle diameters are studied 6 nm and 8 nm. Previous characterization of these samples is reported in Ref. [9], where a notable result is that the temperature for the maximum (T_{\max}) in the low field ZFC magnetization curves of the two highly concentrated samples occurs at around the same temperature (≈ 145 K), whereas the blocking temperatures of the diluted samples were very different, 12.5 and 35 K for the 6 and 8 nm particles, respectively. Here we present results from relaxation experiments, which reveal that the dynamics in the low temperature phase of these two samples

are remarkably different. It is found that the influence of aging on the relaxation, the memory effect, and the apparent spin dimensionality of the two samples are governed by the anisotropy energy barrier of the particles.

II. EXPERIMENTS

Highly monodisperse batches of γ -Fe₂O₃ nanoparticles of 6 and 8 nm were synthesized using the thermal decomposition route described in Refs. [10,11]. The coating of oleic acid on the particles was removed by washing and the solutions were dried yielding powders of NPs. Fractions of the individual powders were pressed into disks using a hydraulic press (0.7 GPa), resulting in two very dense random assemblies which will be referred to as RCP6 (6 nm particles) and RCP8 (8 nm particles). To allow studies of the single particle behavior, two reference samples were made from the same synthesis batches using particles that had subsequently been coated with thick silica shells. These particles were pressed to pellets where the magnetic particle cores were separated far enough to make the dipolar interaction negligible. These reference samples will be referred to as REF6 and REF8.

Magnetization measurements were performed using a custom built low-field SQUID magnetometer [12] as follows.

(i) The magnetization of RCP6 and RCP8 was measured as a function of temperature in a zero-field-cooled (ZFC) protocol using an applied field H of 40 A/m (0.5 Oe). The sample was cooled in zero field from T_{ref} (200 K) in the superparamagnetic state to the lowest temperature ($T_0 \approx 25$ K), where the magnetic field is applied and the magnetization, $M_{ZFC}(T)$, recorded during heating with a fixed rate.

(ii) Zero-field-cooled magnetic relaxation measurements were performed after cooling the systems in zero magnetic field from T_{ref} to the measurement temperature T_m . The system is held at T_m for a wait time t_w , after which a weak magnetic field (40 A/m) is applied and the magnetic relaxation $M_{ZFC}(t)$ recorded vs time, t . After the last measurement point the sample is heated back to T_{ref} , where a reference value of the magnetization is recorded. The relaxation experiments

*Mikael.Andersson@angstrom.uu.se

were repeated using three different wait times $t_w = 0, 300,$ and 3000 s and three different temperatures $T_m = 50, 80,$ and 110 K.

(iii) dc-memory experiments were performed using the protocol described in Ref. [13]. As in ZFC measurements, the sample is cooled in zero field; however, a halt is made at a specific temperature, $T_h < T_g$, for a duration of $t_h = 10000$ s, after which the cooling is resumed down to T_0 . At this temperature the magnetic field is applied and the magnetization is recorded upon heating as in a standard $M_{ZFC}(T)$ measurement. This memory curve is then compared to a reference $M_{ZFC}(T)$ curve recorded without the halt.

(iv) The temperature dependence of an induced isothermal remanent magnetization (IRM) was recorded in a protocol in which the sample is cooled in zero field from T_{ref} to the halt temperature (T_h) where a stop is performed for a time t_h during which a weak field (40 A/m) is applied; after $t_h = 300$ s the magnetic field is switched off and the cooling is resumed down to T_0 . The magnetization is then recorded in zero magnetic field during a subsequent heating (a full description of the IRM protocol is found in Ref. [14]).

III. RESULTS AND DISCUSSION

The main frame of Fig. 1 shows the ZFC magnetization in reduced units as a function of temperature for RCP6 and RCP8 in an applied field of 40 A/m. The lower inset of Fig. 1 shows the out-of-phase component of the ac susceptibility of

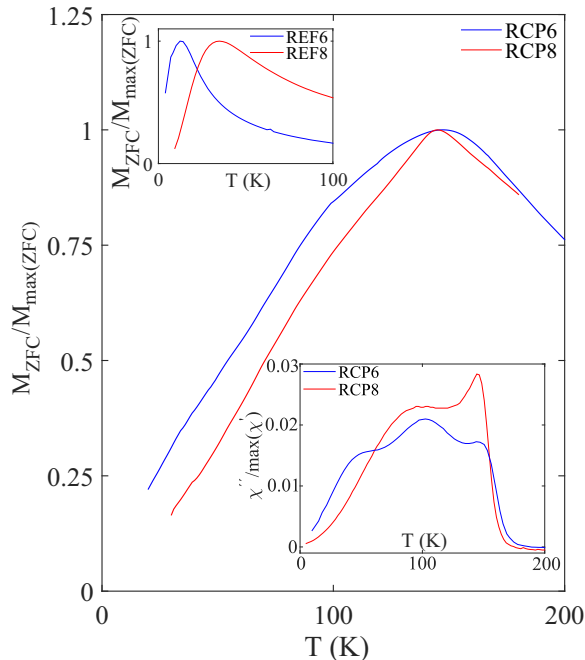


FIG. 1. ZFC magnetization as a function of temperature ($H = 40$ A/m) for the superspin glasses RCP6 and RCP8; data for RCP8 is adapted from Ref. [15]. The upper inset shows the corresponding magnetization for the noninteracting reference samples REF6 and REF8 ($H = 400$ A/m; data adapted from Ref. [9]). The lower inset shows the temperature dependence of the out of phase component of the low field ac susceptibility at 10 Hz of RCP6 and RCP8; adapted from Ref. [16].

RCP6 and RCP8 as a function of temperature, where similarly sharp onsets near T_{\max} are observed in both systems [16]. ZFC magnetization data for REF6 and REF8 recorded in an applied field of 400 A/m (5 Oe) is shown in the upper inset of Fig. 1 and data was recorded using a Quantum Design MPMS; see Ref. [9]. As can be seen, there is a tremendous increase in the temperature of the maximum in the ZFC-magnetization curves when comparing the dilute (REF) samples (i.e., T_b values) with the very dense (RCP) samples (i.e., the T_{\max} values). It can also be seen that T_{\max} for both RCP samples is about the same, 145 K, while T_b for REF6 is 12.5 K and for REF8 is about 35 K. The latter difference is due to the fact that T_b is controlled by the single particle property anisotropy energy barrier, KV . T_{\max} in the RCP samples is instead determined by the strength of the interparticle interaction causing collective behavior of the particle relaxation ($T_{\max} \sim T_g$).

The different values of T_b imply that the energy barrier for REF6 is much smaller than for REF8. Using the Arrhenius expression $\tau = \tau_0 e^{KV/k_B T}$ the energy barrier ($E_a = KV$) is estimated to be 4.6×10^{-21} J for REF6 and 1.3×10^{-20} J for REF8 (cf. Ref. [9]). These values imply individual particle relaxation times (assuming that $\tau_0 = 1 \times 10^{-10}$ s), at 50, 80, and 110 K, of 8×10^{-8} , 6×10^{-9} , and 2×10^{-9} s for RCP6 and 2×10^{-2} , 1×10^{-5} , and 5×10^{-7} s for RCP8, respectively.

The large difference in the temperature evolution of the individual relaxation times between the 6 nm and the 8 nm particles implies that the magnetization on the observation time scale of $M_{ZFC}(T)$ (~ 30 – 100 s) is different for RCP6 and RCP8. Such differences are observed in Fig. 1, where it can be seen that M_{ZFC}/M_{\max} is larger at low temperature for RCP6. This implies that the relaxation rate of the collective dynamics of the magnetization is largely controlled by the individual relaxation time of the particles.

Direct measurements of the relaxation of the ZFC magnetization give quantitative measures of the indirect observations derived from $M_{ZFC}(T)$. Relaxation measurements were made at 50, 80, and 110 K using wait times 0, 300, and 3000 s; the results are presented in Fig. 2, where it can be seen that both systems show aging behavior (t_w dependence; see Refs. [15,17]) at all three temperatures and that the relaxation rate here defined as $S(t) = dM/d \log_{10}(t)$ shows a maximum around t_w . While relaxation rate curves are similar at $T = 110$ K for RCP6 and RCP8 for similar t_w , RCP6 systematically shows higher relaxation rates, $S(t)$, at 80 and 50 K. The ratio of $M_{RCP8}(t=1)/M_{RCP6}(t=1)$ in reduced magnetization is 0.75, 0.93, and 0.95 at 50, 80, and 110 K, respectively.

To further contrast the nonequilibrium dynamics of the two RCP samples, dc-memory experiments were performed at 50, 80, and 110 K, the results of which are plotted in Fig. 3. Both samples show pronounced dips in the memory curves at the halt temperatures, evidencing that the equilibration or aging which occurred during the halts (illustrated in Fig. 2) was kept in memory by the system [13]. There are however significant differences in both magnitude and temperature dependence of the dips as is most clearly seen from the difference plots in the lower panels of Fig. 3. The memory dips of RCP6 are deeper than the memory dips of RCP8, especially at 50 K. Also, the temperature dependence of the depth of the dips is different

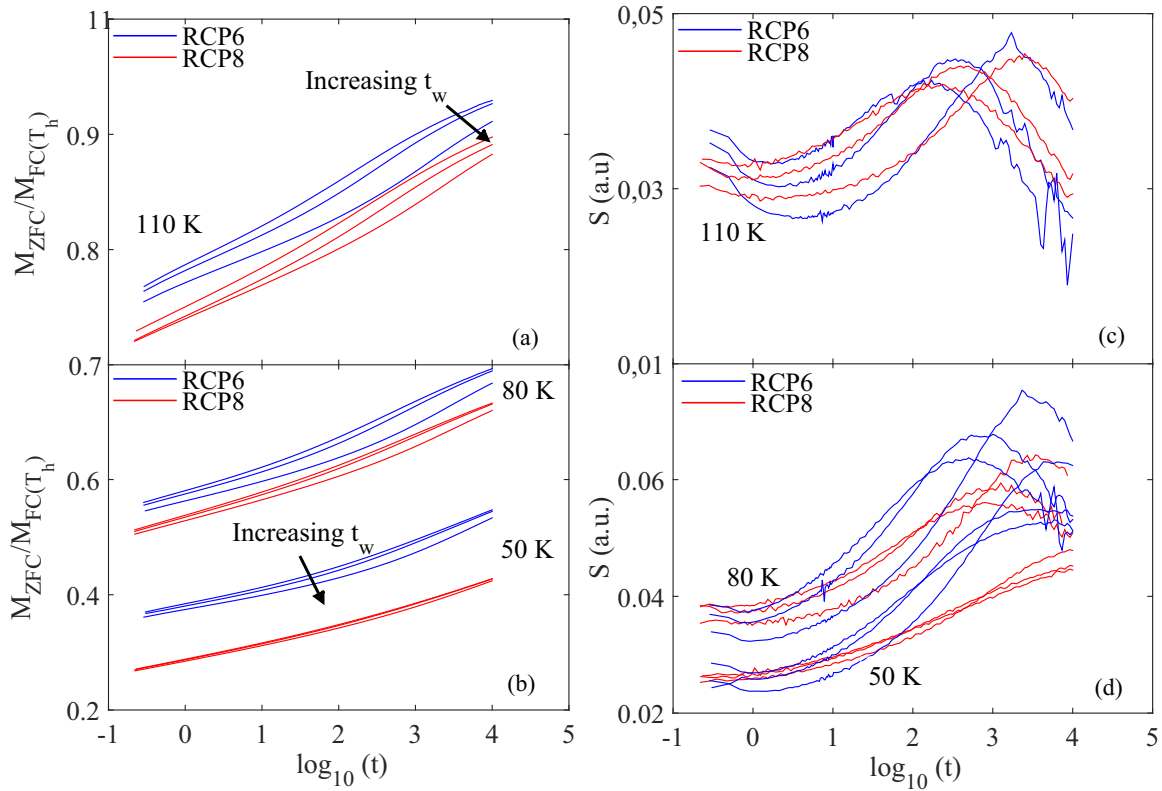


FIG. 2. ZFC magnetic relaxation, $M_{ZFC}(t)$, at wait times $t_w = 0, 300,$ and 3000 s for RCP6 and RCP8 at (a) 110 K and (b) 80 and 50 K; and corresponding relaxation, $S(t)$, rate curves at (c) 110 K and (d) 50 and 80 K. Data for RCP8 is adapted from Ref. [15].

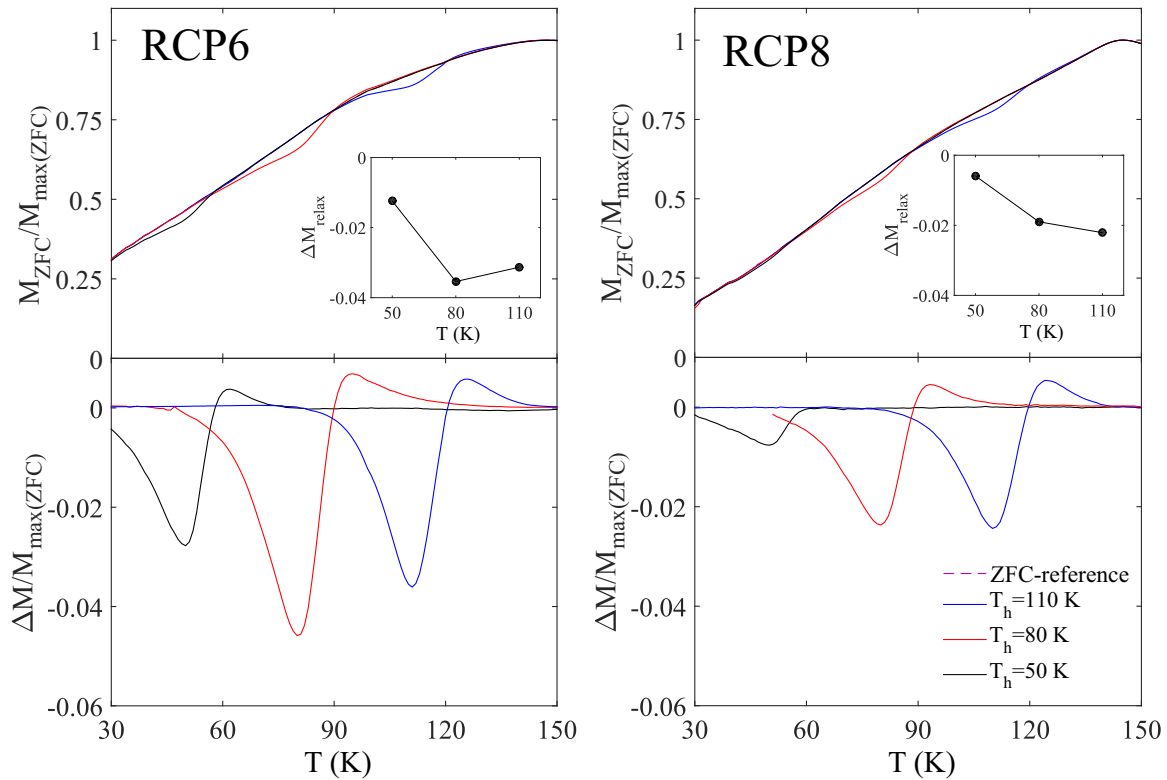


FIG. 3. ZFC memory curves ($H = 40$ A/m) after halting for 10 000 s at either 50, 80, or 110 K and the corresponding reference ZFC curve for both (a) RCP6 and (b) RCP8. Insets show $\Delta M_{Relax} = M(t_w = 3000) - M(t_w = 0)$ at $t = 100$ s from Fig. 2. Data for RCP8 is adapted from Ref. [15].

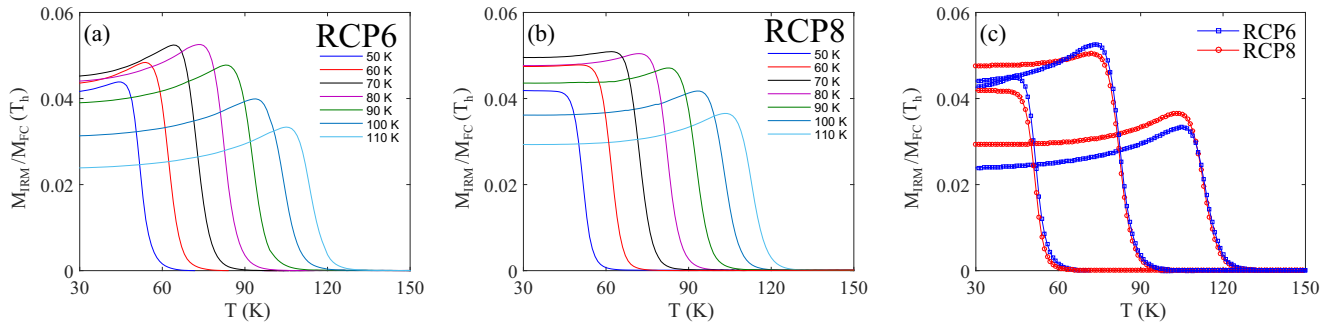


FIG. 4. M_{IRM} vs temperature using a perturbation field of 40 A/m and $t_h = 300$ s for several halting temperatures; $T_h = 50, 60, 70, 80, 90, 100,$ and 110 K for (a) RCP6 and (b) RCP8. (c) Selected $M_{IRM}(T)$ curves for RCP6 and RCP8 plotted together. Data for RCP8 is adapted from Ref. [15].

for the two systems: for RCP6 the largest depth is observed at 80 K, while for RCP8 it is observed at 110 K, with the depth of the 80 K dip only marginally smaller. This difference in the nonequilibrium dynamics of RCP6 and RCP8 is reflected in the corresponding relaxation curves $M(t, t_w)$ in Fig. 2, where it can be seen that the difference of the magnetization values $M(t = 100, t_w = 0)$ and $M(t = 100, t_w = 3000)$ at the three temperatures reflects the evolution of the memory dips with temperature of the two samples. This difference [$\Delta M_{Relax} = M(t_w = 3000) - M(t_w = 0)$] is shown in the insets of Fig. 3.

It was reported in Ref. [15] that the apparent superspin dimensionality shows a crossover from Heisenberg-like to Ising-like character with decreasing temperature in RCP8, a result concluded from measurements of the temperature dependence of the induced isothermal remanent magnetization [$M_{IRM}(T)$]. The observation that has been made on model spin glass samples is that the induced $M_{IRM}(T)$ remains essentially frozen in up to the temperature where it was attained, T_h , and then rapidly decays to zero at higher temperatures. However, when approaching T_h , $M_{IRM}(T)$ has been found to show a maximum for Heisenberg spin glasses but only a smooth decay for Ising spin glasses [14]. The results of such measurements on RCP6 and RCP8 are presented in Fig. 4. Figure 4(a) shows the results for RCP6 using several different temperatures T_h and as can be seen all curves show a maximum before the decay at T_h , indicating a Heisenberg-like nature of the superspins at all measured temperatures. In Fig. 4(b), $M_{IRM}(T)$ of RCP8 is plotted and it can be seen that there is no increase around T_h at low temperatures while at higher temperatures an increase appears, indicating a crossover from an Ising-like to a Heisenberg-like behavior of the superspin. In Ref. [15] it was suggested that an Ising-like character of the NP superspin will be found at relatively high ratios of the anisotropy barrier to the thermal energy, $KV/k_B T$. This idea is confirmed by the data presented in Fig. 4, where the more anisotropic NPs in RCP8 yield a crossover from Ising-like to Heisenberg-like IRM behavior at higher temperatures than those in the RCP6 system, for which no crossover is observed in the studied temperature regime.

Critical slowing down analyses [18,19] of freezing temperatures $T_f(f)$ derived from ac-susceptibility measurements (τ/τ_0 scaling with $[T_f(f) - T_g]/T_g$; $\tau \sim 1/\omega = 1/2\pi f$) showed that both RCP6 and RCP8 undergo a superspin glass transition [16]. A universal behavior of the phase transition was

observed, with critical exponent product $z\nu$ around 8 ± 1 for RCP samples of different sizes. We have reanalyzed that data in the case of RCP6 and RCP8 using the same fixed value of the exponent $z\nu$ in order to compare the microscopic relaxation time τ_0 of the two samples. We find that the microscopic relaxation time of RCP8 is always significantly larger than that of RCP6, e.g., with $z\nu = 8$, $\tau_0 = 5 \times 10^{-9}$ s for RCP8 and $\tau_0 = 2 \times 10^{-11}$ s for RCP6. This difference in τ_0 is in accordance with the larger magnetic anisotropy energy of the larger particles and the evolution of the particle relaxation times according to the Arrhenius law.

IV. CONCLUSIONS

The dynamical magnetic properties of superspin glasses are, in contrast to those of atomic spin glasses, partly controlled by a temperature dependent microscopic relaxation time. In dilute nanoparticle systems the effects of competing dipolar interaction is too weak to introduce spin glass characteristics; thus the behavior is controlled by the evolution of the particle relaxation times according to the Arrhenius law and blocking of the particle moments at low temperatures. With increasing particle concentration and dipolar interaction, the apparent blocking/freezing temperature increases and collective phenomena are introduced in the system. At higher concentrations of particles, the freezing temperature may exceed the blocking temperature by a factor of two or more. In these systems, superspin glass nature of the dynamics is introduced implying nonequilibrium characteristics of the low temperature dynamics including aging, memory, and rejuvenation behavior. In this study we have found that the dynamics of the two superspin glass systems RCP6 and RCP8 exhibit all spin glass characteristics with similar T_g , but the detailed behavior of the temperature dependence of the ZFC magnetization, the magnitude of the aging and memory phenomenon, the temperature for a crossover from Ising to Heisenberg character of the particles, and the relaxation time parameter in critical slowing down are all controlled by the evolution of the relaxation time of the individual particles with temperature.

ACKNOWLEDGMENTS

Financial support from the Swedish Research Council (VR), The Institute of Bioengineering and Nanotechnology

(Biomedical Research Council, Agency for Science, Technology and Research, Singapore), and from the Junta de Comunidades de Castilla-La Mancha (Grant No. PEII-2014-042-P)

is acknowledged. M.S.A. acknowledges the support from K G Westmans stipendiestiftelse.

-
- [1] P. E. Jönsson, in *Advances in Chemical Physics*, edited by S. A. Rice (John Wiley & Sons, Inc., Hoboken, NJ, 2004), pp. 191.
- [2] L. Néel, *Ann. Géophys.* **5**, 99 (1949).
- [3] S. Mørup, M. F. Hansen, and C. Frandsen, *Beilstein J. Nanotechnol.* **1**, 182 (2010).
- [4] K. Hiroi, K. Komatsu, and T. Sato, *Phys. Rev. B* **83**, 224423 (2011).
- [5] K. Hiroi, H. Kura, T. Ogawa, M. Takahashi, and T. Sato, *Appl. Phys. Lett.* **98**, 252505 (2011).
- [6] O. Kaman, T. Koínková, Z. Jiráček, M. Maryško, and M. Veverka, *J. Appl. Phys.* **117**, 17C706 (2015).
- [7] S. Mørup, *Europhys. Lett.* **28**, 671 (1994).
- [8] M. F. Hansen and S. Mørup, *J. Magn. Magn. Mater.* **184**, L262 (1998).
- [9] M. S. Andersson, R. Mathieu, S. S. Lee, P. S. Normile, G. Singh, P. Nordblad, and J. A. De Toro, *Nanotechnology* **26**, 475703 (2015).
- [10] J. A. De Toro, S. S. Lee, D. Salazar, J. L. Cheong, P. S. Normile, P. Muñoz, J. M. Riveiro, M. Hillenkamp, F. Tournus, A. Tamion, and P. Nordblad, *Appl. Phys. Lett.* **102**, 183104 (2013).
- [11] T. Hyeon, S. S. Lee, J. Park, Y. Chung, and H. B. Na, *J. Am. Chem. Soc.* **123**, 12798 (2001).
- [12] J. Magnusson, C. Djurberg, P. Granberg, and P. Nordblad, *Rev. Sci. Instrum.* **68**, 3761 (1997).
- [13] R. Mathieu, P. Jönsson, D. N. H. Nam, and P. Nordblad, *Phys. Rev. B* **63**, 092401 (2001).
- [14] R. Mathieu, M. Hudl, P. Nordblad, Y. Tokunaga, Y. Kaneko, Y. Tokura, H. A. Katori, and A. Ito, *Philos. Mag. Lett.* **90**, 723 (2010).
- [15] M. S. Andersson, J. A. De Toro, S. S. Lee, R. Mathieu, and P. Nordblad, *EPL (Europhys. Lett.)* **108**, 17004 (2014).
- [16] M. S. Andersson, R. Mathieu, P. S. Normile, S. S. Lee, G. Singh, P. Nordblad, and J. A. De Toro (unpublished).
- [17] T. Jonsson, J. Mattsson, C. Djurberg, F. A. Khan, P. Nordblad, and P. Svedlindh, *Phys. Rev. Lett.* **75**, 4138 (1995).
- [18] D. S. Fisher and D. A. Huse, *Phys. Rev. B* **38**, 386 (1988).
- [19] K. Binder and A. P. Young, *Rev. Mod. Phys.* **58**, 801 (1986).